

California AHMCT Program
University of California at Davis
California Department of Transportation

**A BRIDGE-HEIGHT SENSING AND
DATABASE MANAGEMENT SYSTEM FOR
RELIABLE AND EFFICIENT OVERSIZE
PERMITTING AND ROUTING***

Kin S. Yen¹, Travis Swanston¹,
Jagannath Hiremagalur¹, Bahram Ravani¹, &

Ty A. Lasky¹, Principal Investigator

AHMCT Research Report
UCD-ARR-05-02-28-01

Final Report of Contract IA 65A0131

February 28th, 2005

Affiliations:

1. AHMCT Research Center, Department of Mechanical & Aeronautical Engineering, University of California, Davis, CA 95616-5294

* This report has been prepared in cooperation with the State of California, Business Transportation and Housing Agency, Department of Transportation, and is based on work supported by Contract Number IA 65A0131 through the Advanced Highway Maintenance and Construction Technology Research Center at the University of California at Davis.

Technical Documentation Page

1. Report No. CA08-0256	2. Government Accession No.	3. Recipient's Catalog No.	
4. Title and Subtitle A Bridge-Height Sensing and Database Management System for Reliable and Efficient Oversize Permitting and Routing		5. Report Date February 28 th , 2005	
		6. Performing Organization Code	
7. Author(s): Kin S. Yen, Travis Swanston, Jagannath Hiremagalur, Bahram Ravani, & Ty A. Lasky		8. Performing Organization Report No. UCD-ARR-05-02-28-01	
9. Performing Organization Name and Address AHMCT Research Center UCD Dept of Mechanical & Aeronautical Engineering Davis, California 95616-5294		10. Work Unit No. (TRAIS)	
		11. Contract or Grant IA 65A0131	
12. Sponsoring Agency Name and Address California Department of Transportation Sacramento, CA 95819		13. Type of Report and Period Covered Final Report March 2002 - February 2005	
		14. Sponsoring Agency Code	
15. Supplementary Notes			
16. Abstract This report presents STRUCTVIEW, a vehicle-based system for the measurement of roadway structure profiles, which uses a scanning laser rangefinder to measure various structure and roadway features while traveling at highway speed. Measurement capabilities include horizontal and vertical clearances which can be used to support issuing permits based on vehicle height.			
17. Key Words Bridge profile, Clearance measurement, Structure maintenance, Highway maintenance, STRUCTVIEW		18. Distribution Statement No restrictions. This document is available to the public through the National Technical Information Service, Springfield, Virginia 22161.	
20. Security Classif. (of this report) Unclassified	20. Security Classif. (of this page) Unclassified	21. No. of Pages 42	22. Price

Form DOT F 1700.7 (872)
(PF V2.1, 6/30/92)

Reproduction of completed page authorized

Abstract

This report presents STRUCTVIEW, a vehicle-based system for the measurement of roadway structure profiles, which uses a scanning laser rangefinder to measure various structure and roadway features while traveling at highway speed. Measurement capabilities include horizontal and vertical clearances which can be used to support issuing permits based on vehicle height.

Table of Contents

Abstract	iii
Table of Contents	v
List of Figures	vii
Disclaimer/Disclosure	ix
Acronyms and Abbreviations	xi
Acknowledgments	xiii
1 Introduction	1
2 The STRUCTVIEW Concept	5
3 STRUCTVIEW Hardware	9
3.1 Laser Rangefinding Unit	9
3.2 Coaxial Spinning Mirror with Encoder	10
3.3 Radar Speed Sensor	10
3.4 GPS	11
3.5 Human-Machine Interface (HMI)	12
3.6 Camera	12
3.7 Computing, Power, and Communications	12
4 STRUCTVIEW Software	15

4.1	Sensor Application	15
4.2	User Application	15
5	Conclusions and Future Work	21
	References	25

List of Figures

2.1	The profile sensing system and its block diagram.	5
2.2	STRUCTVIEW scan geometry of a simple structure as viewed from behind. Sample STRUCTVIEW profile dimensions are indicated.	6
2.3	STRUCTVIEW scan geometry of a simple structure. The helical nature of the scan data is shown by the purple helix, and the scan axis is indicated by the green arrows. The sample spacing (from sample S_i to S_{i+1}) is exaggerated in the illustration.	6
2.4	Sample California Department of Transportation (Caltrans) roadway clearance diagram [6].	7
3.1	The scanning laser rangefinder.	10
4.1	User application screenshot.	16
4.2	Close-up view illustrating paint stripe identification. The red points depict laser range samples, and the search window is a heuristic device used in the detection process.	17
4.3	Triangle Δabc from a triangulated paint stripe is mapped into the xz plane along with candidate points \mathcal{U} from the overhead structure and \mathcal{V} from the road surface. Points in \mathcal{U} and \mathcal{V} whose corresponding mappings are found to be convex combinations of $(\tilde{a}, \tilde{b}, \tilde{c})$ are known to project vertically through Δabc . y -values from these points are then used to determine the minimum vertical clearance above Δabc	18

Disclaimer/Disclosure

The research reported herein was performed as part of the [Advanced Highway Maintenance & Construction Technology](#) (AHMCT) Research Center, within the Department of Mechanical and Aeronautical Engineering at the University of California Davis, and the Division of Research and Innovation at the California Department of Transportation. It is evolutionary and voluntary. It is a cooperative venture of local, State and Federal governments and universities.

The contents of this report reflect the views of the authors who are responsible for the facts and the accuracy of the data presented herein. The contents do not necessarily reflect the official views or policies of the State of California, the Federal Highway Administration, or the University of California. This report does not constitute a standard, specification, or regulation.

Acronyms and Abbreviations

Acronyms used within this document are defined below.

AASHTO	American Association of State and Highway Transportation Officials
AHMCT	Advanced Highway Maintenance & Construction Technology
API	Application Programming Interface
ASCII	American Standard Code for Information Interchange
BDI	Bridge Diagnostics, Incorporated
C/A	coarse acquisition
Caltrans	California Department of Transportation
CDOT	Colorado DOT
CEP	Circular Error Probable
ConnDOT	Connecticut DOT
DC	Direct Current
DOT	Department of Transportation
DRI	Division of Research and Innovation
EIA	Electronic Industries Alliance
FEA	Finite Element Analysis
FHWA	Federal Highway Administration
FOH	first-order hold
GIS	Geographic Information System
GNU	GNU's Not Unix

GPS	Global Positioning System
HDOP	Horizontal Dilution of Precision
HMI	Human-Machine Interface
HSIF	high-speed interface
HTTP	HyperText Transfer Protocol
JPEG	Joint Photographic Experts Group
NDOR	Nebraska Department of Roads
NMEA-0183	National Marine Electronics Association GPS communications standard
OBD-II	On-Board Diagnostics
PVT	position, velocity, and time
RSA	returned signal amplitude
RS-232	EIA serial communications standard
SDK	Software Development Kit
USB	Universal Serial Bus
USDOT	U.S. Department of Transportation
WAAS	Wide Area Augmentation System
WGS-84	World Geodetic System 84

Acknowledgments

The authors thank the [California Department of Transportation](#) (Caltrans) for their guidance and support; in particular, the guidance and review provided by the Bridge Profile System project team and Technical Advisory Group. The authors also acknowledge the dedicated efforts of the AHMCT development team members. Special thanks to Arvern Lofton of the Caltrans [Division of Research and Innovation](#) (DRI), and to the Caltrans [Structures Maintenance](#) Engineers, particularly Rick Jorgensen and Michael Johnson, who have been instrumental in the design of this system.

Chapter 1

Introduction

Accurate data on the vertical clearances of roadway structures is critically important in oversize route planning and to the nation's economy [1]. Horizontal clearance measurements must also be maintained for security and military purposes [20, 16]. Collecting this data can be dangerous or can cause congestion, and is currently performed by engineers working on or adjacent to the roadway. These work crews are subject to significant traffic hazards, and must obtain measurements during available traffic breaks, which can introduce errors. In addition, from a system-wide perspective, clearance information is in many cases incomplete, inaccurate, difficult to maintain, and difficult to access. Finally, maintaining clearance databases often involves several potentially erroneous manual steps between acquiring the data and updating the database. This report presents STRUCTVIEW, a vehicle-based system for the measurement of roadway structure profiles. The sensing system uses a scanning laser rangefinder to measure various structure and roadway features while traveling at highway speed. Measurement capabilities include horizontal and vertical clearances as specified by [American Association of State and Highway Transportation Officials](#) (AASHTO) guidelines [1] and Federal requirements, which can be used to support issuing permits based on vehicle height. STRUCTVIEW addresses safety hazards by removing the workers from the roadway, and communication issues by reducing the number of manual steps involved in updating the database.

The [U.S. Department of Transportation](#) (USDOT) [Federal Highway Administration](#) (FHWA) Saxton Highway Electronics Laboratory performed pioneering research on the application of laser sensing for structure profiling in 1997 [10]. The system provided a one-dimensional (1D) slice of the structure profile from a vehicle-mounted system, at highway speed, using a single-point laser and a wheel-speed sensor integrated to provide longitudinal distance. Vertical sensing accuracy was very high (0.254 cm, 0.1 in); however, it appears that the system did not have a provision for minimizing or accounting for vehicle bounce, so overall accuracy could be degraded in practice. This prototype system was subsequently tested by the [Connecticut DOT](#) (ConnDOT) [17]. In ConnDOT's testing, the prototype structure clearance measurement system was mounted on their existing photolog vehicles, so that clearance data could be obtained during an existing Department of Transportation (DOT) operation. Such combinations, done properly, can introduce sig-

nificant efficiencies into transportation operations and maintenance—in addition, there can be synergies with regard to available sensors and other supporting in-vehicle infrastructure. One advantage of the 1D approach is that a high sampling rate can be used (up to 500 Hz in the ConnDOT tests), resulting in excellent longitudinal resolution (for ConnDOT, down to 4.47 cm (1.76 in) at 22 m/s (50 mi/hr)), more than sufficient to detect most overhead structural features, with the possible exception of some thinner signs.

A similar commercial system, available from Bridge Diagnostics, Incorporated (BDI), (www.bridgetest.com), is discussed by Mystkowski and Schulz [19]. BDI's system, which was field-tested by the [Colorado](#) DOT (CDOT), measures vehicle bounce using an ultrasonic range sensor, thus providing true clearance over the lane stripe. In the cited CDOT testing, due to low sampling rates, vehicle speed was limited to 8 km/hr (5 mi/hr)—at this speed, a rolling lane closure using an attenuator truck (a.k.a. a shadow vehicle) is required. Subsequent versions of the BDI system (currently the ClearanceMaster 3000™) support measurement at highway speed, with a laser sensor sampling rate of 10 kHz, and seven data points per inch at 34 m/s (75 mi/hr). For all 1D systems, multiple passes must be made through the structure to determine approximate minimum clearance. In addition, by nature they cannot provide horizontal clearance information—essential for national defense and homeland security purposes [20, 16].

Fixed three-dimensional (3D) scanners are seeing increased use in transportation applications. Closely related to the current system, the [Nebraska Department of Roads](#) (NDOR) conducted a pilot study using 3D scanning (with a Riegl LMS-Z360) from roadside locations to develop full point-cloud models and determine clearances for 400 structures [25]. Noteworthy, NDOR has also developed automated Internet-based permitting and routing based on their clearance data. The 3D scanner approach is a strong candidate for this and many other applications. For the structure clearance application, one drawback in some situations is that this approach will require multiple scan locations near the structure to develop the full 3D model needed, and it is often difficult to establish enough safe scanning locations protected from traffic and other hazards; however, the scan locations should still be safer than the current practice of measuring directly on the lanes with or without a lane closure. In addition, to register (or correlate) the multiple scans, it is usually necessary to place known targets (e.g. high-reflectivity spheres) in the scene at locations that will be visible from all planned scan locations, although this requirement is becoming less of an issue as 3D scanning technology evolves. The method does provide very high accuracy (the NDOR study verified vertical clearance accuracies to approximately 3.2 mm (1/8 inch)), and a full 3D model of the structure (thus supporting both vertical and horizontal clearance determination)—such a model will have uses beyond clearance determination, e.g. structure visualization. Jaselskis *et al.* [14] provides an excellent overview of transportation applications for 3D scanning, including a pilot study performed for the Iowa DOT using a Cyrax 2500 scanning unit. Optech Incorporated (www.optech.ca) applied their ILRIS-3D scanner and InnovMetric's PolyWorks™ software in a pilot study for the Florida DOT to investigate the effectiveness of 3D scanning for bridge deflection analysis [22]. Boehler and Marbs [3] overview 3D laser scanning instruments, while Boehler *et al.* [4] overview 3D scanning software. Boehler *et al.* [5]

present a detailed study of laser scanner accuracy; the results of their study, that of Jaselskis *et al.* [14], and our experimental results all indicate that fixed or mobile 3D laser scanning is an ideal candidate for the structure profile application.

Several companies offer software for visualization and manipulation of data obtained using 3D laser scanners. While there are several categories, including scanner control, surface model generation, and data and project management [4], the category of greatest relevance to the current system is point cloud treatment. Point cloud processing software includes, for example (all TM or © of their respective owners), PolyWorks from InnovMetric Software [12], Cyclone CloudWorx from Leica Geosystems [18], and RealWorks Survey from Trimble [26]. Point cloud software typically performs the following tasks: visualization, data cleaning in single point clouds, data filtering and point thinning, registration, data cleaning in registered point clouds, point thinning after registration, and generation of simple plots derived from point clouds [4].

In this report we present the first phase research and development of an alternate approach to the measurement of roadway structure profiles, STRUCTVIEW, which matches the speed, safety, and cost of the current 1D solutions, yet produces a 3D model that can be used to measure features that previously required the use of a stationary 3D scanner or the deployment of a survey crew onto the roadway. STRUCTVIEW operation is at highway speed, eliminating the need for road closures and the associated congestion. This system was developed by the [Advanced Highway Maintenance & Construction Technology](#) (AHMCT) Research Center to meet the needs of the [California Department of Transportation](#) (Caltrans), particularly their Structures Maintenance engineers who are responsible for obtaining structure clearance data, and Traffic Operations, which uses structure profile data for permitting and route planning for vehicles with oversize loads.

Chapter 2

The STRUCTVIEW Concept

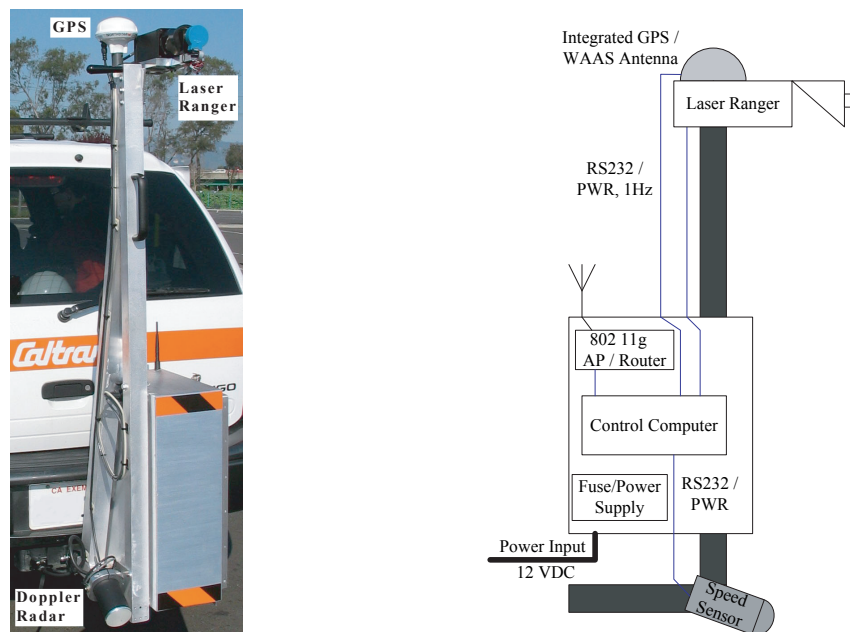


Figure 2.1: The profile sensing system and its block diagram.

The STRUCTVIEW sensing system, shown in Figure 2.1, is a self-contained unit which attaches to the rear of the host vehicle via standard trailer-mount receptacle and power—STRUCTVIEW is highly portable among vehicles of different types, supporting sharing among DOT districts, with resultant cost benefits. Operation is at highway speed and is controlled wirelessly from within the vehicle with a laptop computer. The sensing system employs a laser rangefinding unit with a coaxial spinning mirror oriented to continuously sweep the beam in the plane normal to the vehicle's axis of travel. With the vehicle in motion, this results in a helical scan pattern with screw axis (z) aligned along the roadway. 3D fixes for objects in the beam path are acquired in a cylindrical coordinate system (r, θ, z) (see Figure 2.2 and Figure 2.3 on the next page) with data obtained from three primary sensors. Data from the laser rangefinder is used to determine radial

distance r , angular data from a rotary encoder fixed to the shaft of the spinning mirror is used to determine polar angle θ , and vehicle speed v from a ground-speed radar sensor is integrated to calculate z . STRUCTVIEW also collects geospatial coordinates of sampled structures using a differential Global Positioning System (GPS) receiver, and, optionally, captures a series of photographs of each structure via a dash-mounted digital camera connected to the Human-Machine Interface (HMI) laptop. The system assumes there is no vehicle pitch or roll (small angles will introduce minimal errors). As STRUCTVIEW uses a local relative measurement technique, vehicle bounce (along y) and lateral offsets (along x) will not significantly affect the profile data; however, these factors will influence the resulting 3D point cloud, and this must be considered in any subsequent use of this point cloud for measurements not targeted by STRUCTVIEW.

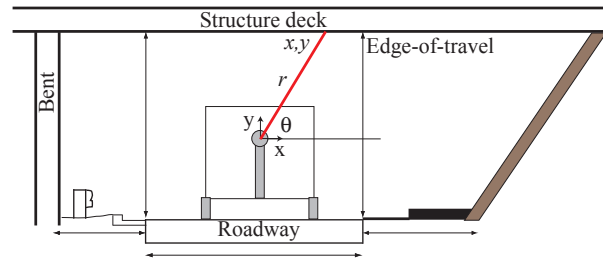


Figure 2.2: STRUCTVIEW scan geometry of a simple structure as viewed from behind. Sample STRUCTVIEW profile dimensions are indicated.

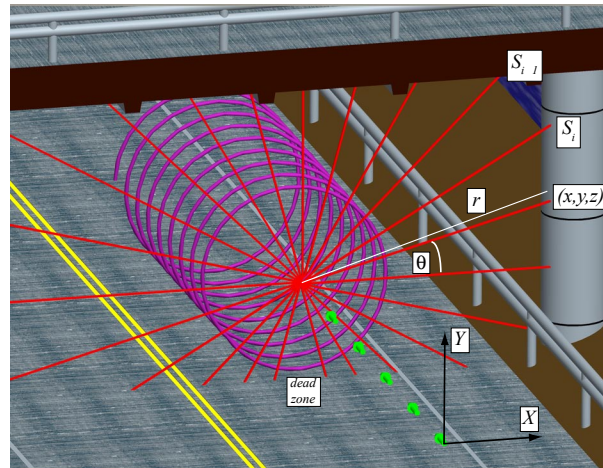


Figure 2.3: STRUCTVIEW scan geometry of a simple structure. The helical nature of the scan data is shown by the purple helix, and the scan axis is indicated by the green arrows. The sample spacing (from sample S_i to S_{i+1}) is exaggerated in the illustration.

In use, the vehicle is driven to sample a series of structures, with the raw data collected on the HMI laptop. At the end of the sampling run the laptop is taken back to the office where the data is processed and profile measurements are interactively extracted from each of the sampling sessions. An example clearance diagram is shown in Figure 2.4 on the facing page.

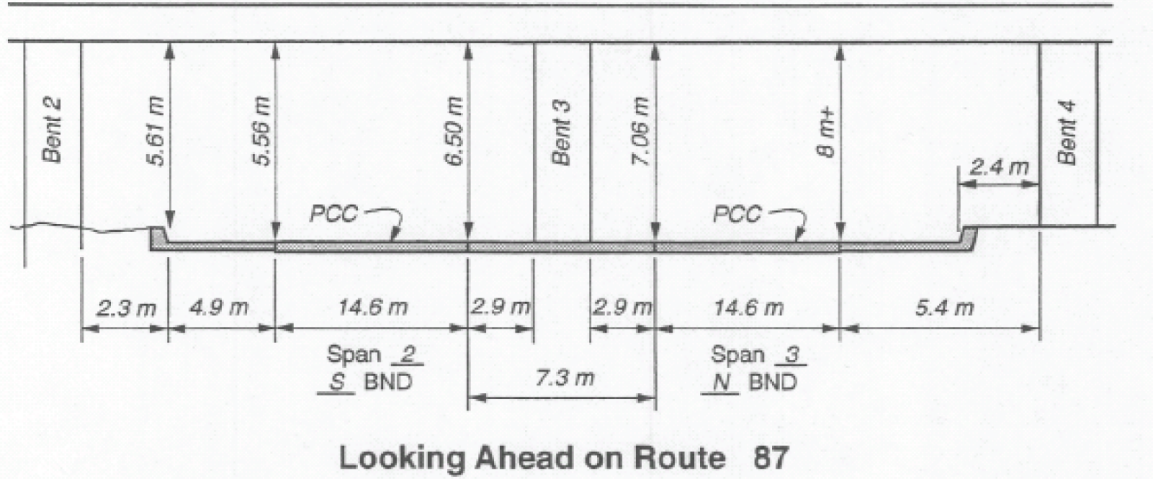


Figure 2.4: Sample Caltrans roadway clearance diagram [6].

STRUCTVIEW is a multirate sampled-data system [2], with high-rate sampling for the laser rangefinder and the encoder (frequency $f_l = f_e = 50$ kHz, period $T_l = T_e = 20 \mu\text{s}$), and low-rate sampling for the ground-speed radar ($f_v = 10$ Hz, $T_v = 100$ ms) and the GPS ($f_g = 1$ Hz, $T_g = 1$ s). The sampled-data signals, denoted for example as $r^*(t)$, are the impulse series signals corresponding to the continuous signals, e.g. $r(t)$, at time kT_i ($i = l, e, v, g$), so that, for example,

$$r^*(t) = \sum_{k=0}^{\infty} r(kT_l) \delta(t - kT_l) \quad (2.1)$$

For the low-rate data (GPS and ground-speed radar), a non-causal first-order hold (FOH) is used to linearly interpolate between samples. For example, the low-rate radar ground-speed data is interpolated in this manner to obtain the longitudinal dimension, z , as

$$z(t) = - \int_{t_0}^t v(\tau) d\tau, \text{ or } z^*(kT_l) = -T_l \sum_{i=0}^k \text{FOH}(v^*(iT_l)) \quad (2.2)$$

Here, t_0 is the starting time for each scan (i.e., the integration is reset for each scan to remove error accumulation), $\text{FOH}()$ denotes the non-causal first-order hold operation, and v is obtained from the ground-speed sensor based on equation (3.1). Based on the Cartesian frame used (see Figure 2.3 on the preceding page), z will always be negative.

The system maintains both cylindrical and Cartesian coordinates. To complete the localized Cartesian coordinates, data is converted from the natural polar coordinates of the laser rangefinder and encoder (see Figure 2.2 on the facing page) at rate f_l as

$$(x^*(t), y^*(t)) = r^*(t)(\cos \theta^*(t), \sin \theta^*(t)) \quad (2.3)$$

Chapter 3

STRUCTVIEW Hardware

Figure 2.1 on page 5 provides an overview of the core hardware components, which will be discussed in detail in this chapter. The photo shows the STRUCTVIEW prototype hardware mounted on a research vehicle, requiring only a standard trailer mount receptacle and connection to the vehicle 12-volt power via standard trailer power connector, so that STRUCTVIEW is highly portable among vehicles of different types.

As system portability is an important constraint, the weight of the system was minimized in the design. However, structural rigidity was important, based on the sensing accuracy requirements. Finite Element Analysis (FEA) was used to optimize the weight vs. rigidity. The detailed FEA study is not included here. Additional weight optimization is occurring in ongoing research efforts. In particular, now that STRUCTVIEW prototype component selection is final, improvements can be achieved by reducing the electronics enclosure's size and weight.

3.1 Laser Ranging Unit

The scanning laser rangefinder is the primary STRUCTVIEW sensor; the prototype uses a factory-modified version of the Acuity Research (Schmitt Measurement Systems, Inc.) AR4000-LV, a time-of-flight rangefinder based on a 5 mW 670 nm wavelength visible red laser diode [24]. This Class IIIa sensor provides range $r(t)$ and returned signal amplitude (RSA) $a(t)$ in the 0 - 16.5 m (0 - 54 ft) range. RSA is important as it is used within STRUCTVIEW in the identification of retroreflective paint stripes, and thus for horizontal dimension extraction; it also plays a significant role in STRUCTVIEW's noise filtering. For a general overview of laser range sensors and accuracy characterization, see works by Boehler *et al.* [4, 3, 5].

3.2 Coaxial Spinning Mirror with Encoder

The AR4000-LV, combined with Acuity's AccuRange Line Scanner and high-speed interface (HSIF) card (all TM Schmitt Measurement Systems, Inc.), provides a laser scanner (see Figure 3.1) with circular sweep (provided by a spinning mirror) at $\omega = 272 \text{ rad/s}$ (2600 RPM, 43.3 Hz, 23.1 ms per sweep), with angular position provided by an integrated 4096-count optical encoder (1.534 mrad/count). With laser sweep rate ω and forward vehicle velocity v , the longitudinal resolution (along the road) for the integrated system is given by $\rho_z = 2\pi v/\omega$. As integrated for the structure scanning operation, this sweep rate combined with forward velocity $v = 24.6 \text{ m/s}$ (55 mi/hr) yields $\rho = 0.57 \text{ m}$ (1.9 ft). The combined sensing package provides target range r , RSA a , and laser beam angle θ , at sampling rate $f_l = 50 \text{ kHz}$. The line scanner mounting blocks the signal, creating a dead zone of 1.05 rad (60°) directly below the laser with the off-the-shelf mount. STRUCTVIEW uses a modified mount to reduce the dead zone to approximately 0.44 rad (25°). With the sensor mounting height of approximately 1.4 m (4.5 ft), this yields about 0.6 m (2.0 ft) of blocked pavement laterally, varying of course with mount height and vehicle bounce. The mount location was selected to place this dead zone near the center of the driving lane, so that it will not impact STRUCTVIEW operation and output, based on system requirements (height above lane stripes) and operating mode. The laser scanner data, combined with the integrated vehicle velocity, yields a 3D point cloud of the structure and roadway, including RSA, while also retaining the intrinsic helical scan structure exploited in the subsequent processing.



Figure 3.1: The scanning laser rangefinder.

3.3 Radar Speed Sensor

Generally speaking, a vehicle's ground speed and distance traveled can be provided via its built-in sensors, GPS, or other means. Use of built-in vehicle sensors, e.g. via the On-Board Diagnostics (OBD-II) connector, introduces uncertainty in terms of accuracy and calibration, and was not pursued here in order to maximize portability between vehicle types. GPS is also not an appropriate choice for the primary speed sensor in the application, as the satellite signals are blocked while passing through structures. However, structures are typically short (except for tunnels) and speed is generally constant during the scanning process, so simple interpolation of GPS-obtained speed before entering and

after leaving the structure can provide a fair estimate of speed through the structure, allowing GPS to act as a redundant speed sensor. Future work may include more advanced sensor integration via Kalman filtering.

Based on the application requirements and the limitations of built-in speed sensors and GPS, a Doppler radar sensor, the Decatur SI-2, was selected as STRUCTVIEW's primary speed sensor. This sensor operates in the K-band ($f_0 = 24.150 \text{ GHz} \pm 50 \text{ MHz}$), with 0.21 rad (12°) beam width, and 10 mW nominal output power [8]. Sensor range is $3 - 320 \text{ km/hr}$ ($2 - 200 \text{ mi/hr}$), with accuracy of $\pm 0.1 \text{ km/hr}$. Doppler shift is approximately $f_d = 45 \text{ Hz}/(\text{km/hr})$, or $72 \text{ Hz}/(\text{mi/hr})$. The fundamental relation for speed from Doppler shift is [11]

$$v_z(t) = -\frac{c}{2 \cos \theta_{ss}} \left(\frac{f_d(t)}{f_0} \right) \quad (3.1)$$

where c is the speed of light, θ_{ss} is the angle between the horizontal (road) plane and the sensor centerline, and the negative sign is specific to the sensor mounting and choice of z -axis (opposite of travel direction). The SI-2 configuration includes input of θ_{ss} , and the RS-232 interface provides the derived speed in American Standard Code for Information Interchange (ASCII) format. Sensor power ($+12 \text{ V}$) is provided through the EIA serial communications standard (RS-232) DB9 connector.

3.4 GPS

STRUCTVIEW uses a GPS receiver [9] for structure identification and coordination with the DOT's Geographic Information System (GIS) database. The unit is a NovAtel Smart Antenna [21], an integrated antenna and GPS receiver board based on the Superstar II chipset. This receiver provides 12-channel L1-frequency coarse acquisition (C/A) code solution with better than 5 m Circular Error Probable (CEP) accuracy, and carrier phase tracking combined with the Wide Area Augmentation System (WAAS) for differential corrections to achieve better than 1.5 m CEP. This level of accuracy is more than sufficient for the current application and avoids the need for a fixed base station, improving the portability and range of the structure profile assessment system.

The GPS receiver also provides redundant velocity sensing (0.05 m/s RMS) while entering and leaving the structure. The GPS unit provides position, velocity, and time (PVT) in National Marine Electronics Association GPS communications standard (NMEA-0183) format via an RS-232 serial interface. The output data (World Geodetic System 84 (WGS-84) global reference frame) includes latitude $\phi(t)$, longitude $\lambda(t)$, and altitude or height $h(t)$, i.e., the distance from the WGS-84 ellipsoid.

By the very nature of GPS, this sensor is not available while traveling through the structure. Given the functional requirements (structure identification / verification, and redundant velocity sensing at structure end points), this is not a problem in the current application. Structure identification and verification requires only very coarse accuracy and a single-point reading (coordinated with the camera discussed below)—typically the

GPS accuracy greatly exceeds the GIS accuracy for structure records. Also, as the operation is performed at near constant velocity, the speed readings from the GPS receiver on entering and leaving the structure can be interpolated effectively to provide redundant speed approximation while under the structure. The receiver reacquires the satellite signals and navigation tracking quickly on leaving the structure. For system health and accuracy validation, additional data is collected, including the number of visible satellites and Horizontal Dilution of Precision (HDOP).

3.5 Human-Machine Interface (HMI)

The in-vehicle HMI is provided via a laptop computer. This choice was based primarily on user preference as indicated in system design reviews with the DOT—in addition, this choice provides flexibility for research, and allows the operators to perform data analysis in the field, if preferred. The laptop used is a 1.7 GHz Pentium mobile, with an ATI 9600 graphics chipset.

Bi-directional communication between the sensing platform and the HMI is provided via 802.11g (WiFi) [13]. This design decision greatly facilitated vehicle integration. As a result, the only HMI connection that may be needed is to the vehicle's standard 12-volt power adapter, and the sensing platform requires only standard trailer-hitch power. Hence, the total system is easily portable and can be installed on a wide range of vehicles.

3.6 Camera

For structure ID verification, STRUCTVIEW includes a forward-looking dash-mounted digital still camera. The HMI controls the camera using the Canon Universal Serial Bus (USB) Application Programming Interface (API) [7], and transfers images back to the HMI device via the USB port. Currently, the camera is triggered via the **Photo** or **Start** buttons in the HMI, and takes a single snapshot of the structure profile. The resulting [Joint Photographic Experts Group](#) (JPEG) image is stored as part of the database for this structure scan. The camera subsystem is currently being updated to provide a series of images as the support vehicle moves through the structure.

3.7 Computing, Power, and Communications

Power to the sensing platform is provided via a standard trailer hitch connection, again providing portability and easy installation. The sensing platform power input is +12 volt Direct Current (DC), with internal conversion to provide all additional voltages. The device control computer, based on a 1.2 GHz Intel Pentium 3 CPU, with 1 GB RAM, uses a direct DC supply, thus avoiding inverter inefficiencies. The laser sensor uses +5 V, the

GPS uses +12 V, and the ground speed radar uses +12 V. The camera and the HMI laptop are battery-powered, but can also use the in-vehicle 12 V supply if needed.

System communications between the HMI and the sensing computer is via 802.11g wireless [13]. Communications (data and control) between the HMI computer and the still digital camera is over a wired USB connection [7]. Communications within the sensing platform is typically via RS-232, as noted in the detailed discussion for the hardware components.

Chapter 4

STRUCTVIEW Software

The STRUCTVIEW software components were written in C++ and built on Trolltech's Qt™ development framework. Initial development was carried out in a [GNU's Not Unix](#) (GNU) / Linux environment, but Microsoft's Windows XP® was ultimately selected for production, primarily due to the availability of vendor-supplied drivers and Software Development Kits (SDKs) for some of the more proprietary hardware used in the system. The software consists of two packages: the sensor application which runs on the device controller, and the user application which runs on the HMI laptop.

4.1 Sensor Application

The sensor application runs on the device controller and serves as the interface to the system's sensors, coordinating all control and data acquisition activities. At startup, it spawns a dedicated thread for each STRUCTVIEW sensor. Each thread is responsible for all configuration and data acquisition for its sensor, and is controlled by the application via sockets and shared memory. While in its "ready" state, the sensor application waits for and responds to commands issued by the user application. Communication between the sensor platform and the user application on the HMI is by means of an HyperText Transfer Protocol (HTTP)-based protocol. During a sampling session, each thread initializes its sensor and begins to acquire and log data, time-stamping it for later synchronization. Sensor logs for the session are organized into a batch and tagged with a unique identifier. When the session is terminated, the batch is compressed and transferred to the user application.

4.2 User Application

The user application runs on the HMI laptop, handling all user interaction, including configuring the system, performing and organizing sampling sessions, as well as the

subsequent visualization and analysis of acquired data. Sampling sessions can also be annotated with voice or text.

Based on prototype development and initial testing with end users, a simple button-based graphical interface was chosen; however, hot-keys are also available for expert users. A key STRUCTVIEW requirement is the ability to rapidly cycle through the sampling process for closely-spaced structures. Structure spacing is sometimes on the order of 0.4 km (0.25 mile), so at highway speed, there may be as little as 10 - 15 seconds between sampling operations. This can be quite demanding on the user, and significantly impacted the design, driving the need for simplicity and efficient data handling.

After sampling is complete and data has been processed, the user application renders a 3D view of the dataset. The user can then explore, manipulate, and measure a variety of structural features, including the vertical and horizontal clearances specified by AASHTO guidelines [1] and Federal requirements [20, 16]. Minimum vertical clearances are determined above road edges and above each paint stripe, making paint stripe identification an important feature recognition function. An example of such an operation is shown in Figure 4.1.

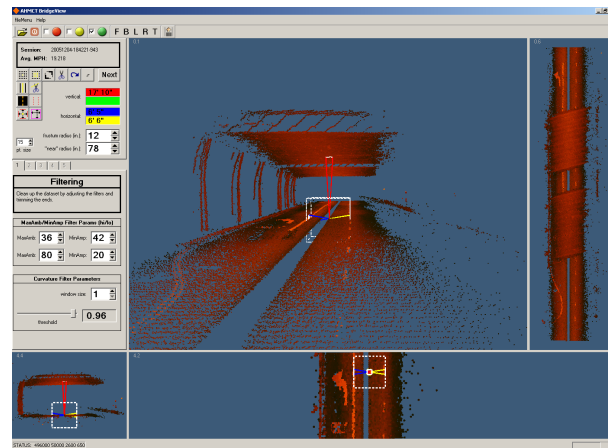


Figure 4.1: User application screenshot.

To support this functionality, the data recorded from each sampling operation passes through a preprocessing stage before the user can interact with it. First, the logs from each sensor (rangefinder/encoder, radar speed sensor, GPS) are parsed and any relevant calibration is applied. These sensors produce data at different rates, so the timestamps recorded during the sampling operation are then used to synchronize the three data streams. The GPS and speed sensor streams are then merged into the much higher-rate rangefinder stream through linear interpolation and resampling, producing a 50 kHz set of datapoints, each point of which contains data reflecting measurements from all three sensors.

Next, various filters are applied to these datapoints to remove noise and other artifacts, including invalid range samples in the dead zone described above. Following this, the datapoints are mapped into a cylindrical coordinate system (r, θ, z) with z aligned

opposite the vehicle's direction of travel (refer to Figure 2.3 on page 6). The r axis represents the range of each point from the sensor, angle θ is derived from the discrete (0-4095) encoder value, and z is an approximation of the longitudinal location of the point from equation (2.2). The origin is defined such that $r = 0$ is the location of the laser rangefinder, $\theta = 0$ is horizontal toward the vehicle's starboard, and $z = 0$ is set at the location of the laser rangefinder at the instant of the first sample taken in the dataset. To enhance the performance of subsequent processing, the points are also mapped into a Cartesian coordinate system. Both of these coordinate systems share the same origin and z axis. The x axis of the Cartesian system is aligned with $\theta = 0$.

Finally, the datapoints are organized into a time-ordered set of "cycle structures", each of which is itself a time-ordered set of datapoints collected during one full (2π rad) sweep of the beam. Arranging the data in this way allows the sample set to be quickly traversed for the detection and identification of features such as paint stripes, curbs and structural and roadway surfaces (Figure 4.2). Without this arrangement there is only a general unordered point cloud, which would require use of computationally expensive surface identification algorithms. For example, one of the tools offered by the user application allows for the interactive identification of paint stripes on the road surface. To do this, the tool needs to be able to quickly traverse the set of datapoints representing the road surface, searching for patterns in the returned signal amplitude that potentially fit the profile of a paint stripe. Using the cycle structures, a raster-like scan of the road surface can be performed by iterating, in order, through the datapoints in each cycle.

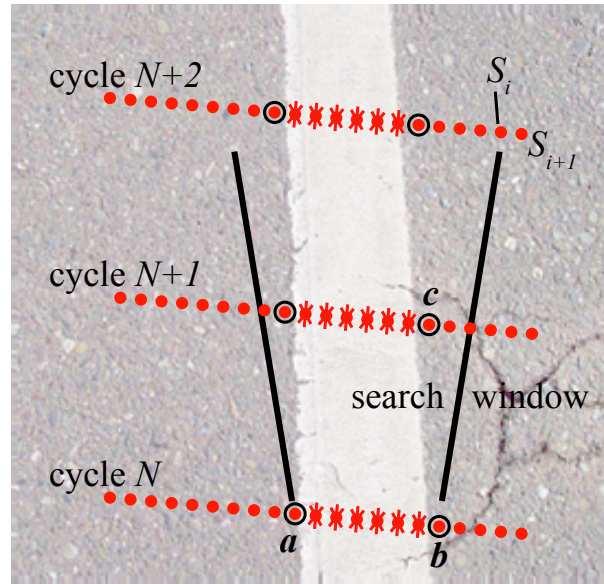


Figure 4.2: Close-up view illustrating paint stripe identification. The red points depict laser range samples, and the search window is a heuristic device used in the detection process.

One of the main requirements of the system is the ability to determine the minimum clearance of an overhead structure (e.g. a bridge) above the lanes on the road or above the paint stripes that divide them. Once the paint stripes and lanes have been identified as

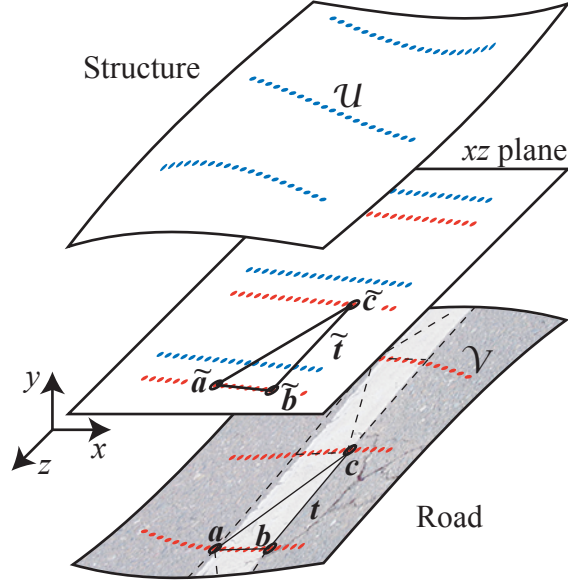


Figure 4.3: Triangle Δabc from a triangulated paint stripe is mapped into the xz plane along with candidate points \mathcal{U} from the overhead structure and \mathcal{V} from the road surface. Points in \mathcal{U} and \mathcal{V} whose corresponding mappings are found to be convex combinations of $(\tilde{a}, \tilde{b}, \tilde{c})$ are known to project vertically through Δabc . y -values from these points are then used to determine the minimum vertical clearance above Δabc .

discussed above, they are triangulated. The resulting set of triangles $\mathcal{T} = \{t_i \mid i \in \mathbb{N}, i \leq n\}$, along with a set of candidate points \mathcal{U} from the overhead structure and a set of candidate points \mathcal{V} from the road surface¹, is then orthographically projected onto the xz plane as shown in Figure 4.3. Now reduced to two dimensions, a point-triangle inclusion test (described below) is performed for each projected triangle $\tilde{t}_i \in \tilde{\mathcal{T}}$ against all the points in projected sets $\tilde{\mathcal{U}}$ and $\tilde{\mathcal{V}}$. Since the point sets $\tilde{\mathcal{U}}_{cc} \subseteq \tilde{\mathcal{U}}$ and $\tilde{\mathcal{V}}_{cc} \subseteq \tilde{\mathcal{V}}$ which pass the \tilde{t}_i inclusion test all lie in or on \tilde{t}_i , it also holds that the vertical projections of those points' corresponding preimages (in $\mathcal{U}_{cc}, \mathcal{V}_{cc}$) must pass through that triangle's preimage, t_i (in \mathcal{T}). The minimum overhead clearance h_i above the triangle t_i is then calculated as the difference between the minimum y -value found among the points in \mathcal{U}_{cc} and the maximum y -value found among the points in \mathcal{V}_{cc} . This process is repeated for each $t_i \in \mathcal{T}$, and the lowest clearance value found is then considered to be the minimum overhead clearance along \mathcal{T} :

$$MOHC(\mathcal{T}) = \min h_i. \quad (4.1)$$

This technique is useful not only in determining minimum vertical clearances, but also anywhere the software needs to perform orthographic distance measurements between sections of surfaces defined by point sets.

¹ \mathcal{U} and \mathcal{V} are the result of a coarse subdivision and culling procedure that separates overhead structure points from road surface points and eliminates most of the points that are not relevant to the clearance calculations.

The 2D point-triangle inclusion test mentioned above is accomplished by considering some given point \mathbf{p} as an affine combination of the points that define a triangle $\Delta\mathbf{abc}$:

$$\mathbf{p} = \lambda_a \mathbf{a} + \lambda_b \mathbf{b} + \lambda_c \mathbf{c} \quad (4.2)$$

$$\lambda_a + \lambda_b + \lambda_c = 1 \quad (4.3)$$

The linear system defined by (4.2) and (4.3) can be solved to yield the coefficients² $(\lambda_a, \lambda_b, \lambda_c)$, which can then be used to classify \mathbf{p} 's relationship to $\Delta\mathbf{abc}$ [23, 15]. One of the properties of these coefficients is that if (and only if) they are all non-negative, then \mathbf{p} lies on or within $\Delta\mathbf{abc}$, i.e.,

$$\mathbf{p} \in \Delta\mathbf{abc} \iff \lambda_a, \lambda_b, \lambda_c \geq 0. \quad (4.4)$$

In other words, \mathbf{p} is a convex combination of $(\mathbf{a}, \mathbf{b}, \mathbf{c})$.

²These coefficients are commonly known as the barycentric coordinates of \mathbf{p} with respect to $\Delta\mathbf{abc}$. The coefficients can be thought of as a coordinate system (barycentric space) for the plane defined by T_{abc} .

Chapter 5

Conclusions and Future Work

STRUCTVIEW provides a vehicle-based approach to obtaining structure profile measurements needed by DOTs for issuing permits based on vehicle height, as well as the horizontal dimensions needed by the military and Homeland Security. It allows sensing at highway speed, and yields a full 3D point cloud. The STRUCTVIEW user application supports extraction of all the required structure profile dimensions in an efficient and cost-effective manner. STRUCTVIEW gets the Structures Maintenance workers off of the roadway and into a safe environment in the host vehicle. In addition, the sensing and analysis workflow removes many of the opportunities for human error inherent in manual data collection and documentation. With the resulting improvement in the accuracy and timeliness of structure profile information and resulting oversize permitting, there will be a lower probability of related bridge strikes, with associated cost, safety, and congestion benefits. Finally, as highway-speed sensing removes the need for fixed or rolling lane closures, the traveling public will not be impacted by the lane closures required by most current approaches. In summary, STRUCTVIEW will enhance the overall mobility of the transportation system.

While STRUCTVIEW provides a significant advance in the state of the art for structure profile assessment, there are areas for future work that are being investigated at the AHMCT Research Center. In the current incarnation, all system function is initiated by the user via the HMI. It is desirable to automate some of the functionality further. For example, sampling could be initiated based on vehicle location using the GPS receiver. Conceptually, this is simple. In practice, based on discussions with the DOT, such an approach is typically impractical to date, as the highway and structure location data in the existing State GIS database is far too inaccurate to support this operating mode; however, the researchers and the DOT are considering improvements to the GIS data. Work is currently in progress to automate generation of complete Caltrans format structure profile diagrams from the processed sensor data. Additional ruggedization and hardware improvements are underway to increase the potential for deployment and field use of the system. Finally, additional improvements in noise reduction and surface recognition are recommended to improve the reliability of the clearance measurement results, followed by additional detailed testing and evaluation by Caltrans.

References

- [1] American Association of State Highway and Transportation Officials. *Manual for Condition Evaluation of Bridges*, 2nd edition, 2000.
- [2] Mituhiko Araki and Koichiro Yamamoto. Multivariable multirate sampled-data systems: State-space description, transfer characteristics, and Nyquist criterion. *IEEE Transactions on Automatic Control*, AC-31(2):145–154, February 1986.
- [3] W Boehler and A Marbs. 3D scanning instruments. In *CIPA Heritage Documentation, International Workshop on Scanning for Cultural Heritage Recording*, pages 9–12, Corfu, Greece, September 2002. URL http://www.i3mainz.fh-mainz.de/publicat/korfu/p05_Boehler.pdf.
- [4] W Boehler, G Heinz, A Marbs, and M Siebold. 3D scanning software: An introduction. In *CIPA Heritage Documentation, International Workshop on Scanning for Cultural Heritage Recording*, pages 47–51, Corfu, Greece, September 2002. URL http://www.i3mainz.fh-mainz.de/publicat/korfu/pl1_Boehler.pdf.
- [5] W Boehler, M Bordas Vicent, and A Marbs. Investigating laser scanner accuracy. In *XIXth CIPA Symposium*, Antalya, Turkey, September 2003. URL http://www.i3mainz.fh-mainz.de/publicat/cipa2003/laserscanner_accuracy.pdf.
- [6] California Department of Transportation. Area Bridge Maintenance Engineer (ABME) structure maintenance procedures. Technical report, Business, Transportation and Housing Agency, January 1995.
- [7] Canon USA. Canon developer support site, 2005. URL www.developersupport.canon.com.
- [8] Decatur Electronics, Inc. Speed interface, SI-2 (regular speed), October 2002. URL www.decaturradar.com.
- [9] Alan G. Evans, Robert W. Hill, Geoffrey Blewitt, Everett R. Swift, Thomas P. Yunck, Ron Hatch, Stephen M. Lichten, Stephen Malys, John Bossler, and James P. Cunningham. The Global Positioning System geodesy odyssey. *ION Journal of Navigation*, 49(1):7–33, 2002.

- [10] FHWA Turner-Fairbanks Highway Research Center. Research & technology transporter on-line: Overpass height measuring goes high tech, September 1997. URL www.tfhrc.gov/trnsptr/rttsep97/tr997p8.htm.
- [11] GMH Engineering. Application note 1000: Fundamentals of non-contact speed measurement using Doppler radar, 2003. URL www.gmheng.com/pdf/an1000.pdf.
- [12] InnovMetric Software Inc. PolyWorks for 3D digitizer and 3D scanner, 2005. URL www.innovmetric.com/Surveying/english/home.html.
- [13] Institute of Electrical and Electronics Engineers Inc. IEEE std 802.11g: Wireless LAN Medium Access Control (MAC) and Physical Layer (PHY) specifications: Further higher-speed physical layer extension in the 2.4 GHz band, 2003.
- [14] Edward J. Jaselskis, Zhili Gao, Alice Welch, and Dennis O'Brien. Pilot study on laser scanning technology for transportation projects. In *Mid-Continent Transportation Research Symposium*, Ames, Iowa, 2003.
- [15] Juan José Jiménez, Rafael J. Segura, and Francisco R. Feito. Efficient collision detection between 2D polygons. *Journal of WSCG*, 12(1–3):191–198, 2004.
- [16] David Keever and Julie Soutuyo. Coordinating military deployments on roads and highways: A guide for state and local agencies (Chapter 3: Typical military deployment movements on public roads). Technical Report FHWA-HOP-05-029, U.S. Department of Transportation Federal Highway Administration, May 2005. URL www.ops.fhwa.dot.gov/OpsSecurity/dev-mx/index.htm#toc.
- [17] Robert G. Lauzon. Automated vertical clearance measurement during photolog operations. Technical Report 2220-F-2000-4, Connecticut Department of Transportation, Bureau of Engineering and Highway Operations, Division of Research, September 2000.
- [18] Leica Geosystems. Cyclone software - where it all “comes together”, 2005. URL http://www.leica-geosystems.com/corporate/en/ndef/lgs_3490.htm.
- [19] W. Mystkowski and J.L. Schulz. Development and use of a laser-based roadway clearance measurement system. In *Proceedings of TRB 8th International Bridge Management Conference*, pages B–11/1–B–11/9, 1999.
- [20] Louis G. Neudorff, Jeffrey E. Randall, Robert Reiss, and Robert Gordon. Freeway management and operations handbook: Final report (Chapter 12: Freeway management during emergencies and evacuations). Technical Report FHWA-OP-04-003, U.S. Department of Transportation Federal Highway Administration, September 2003. URL http://ops.fhwa.dot.gov/freewaymgmt/freeway_mgmt_handbook/toc.htm.
- [21] NovAtel, Inc. Novatel’s smart antenna, 2005. URL www.novatel.ca/Documents/Papers/SMRT_ant.pdf.

- [22] Optech Incorporated. Field notes, civil engineering: Bridge deflection analysis, 2002. URL www.innovmetric.com/Surveying/english/pdf/optech.pdf.
- [23] Joseph O'Rourke. *Computational Geometry in C*. Cambridge University Press, 1998.
- [24] Schmitt Measurement Systems, Inc. Acuity AR4000 laser rangefinder equipment overview, 2005. URL www.acuityresearch.com/products/ar4000/index.shtml.
- [25] Russ L. Tamblyn. Viable viaducts, February 2004. URL www.innovmetric.com/Surveying/english/pdf/viaducts.pdf. Point of Beginning.
- [26] Trimble. RealWorks Survey, 2005. URL www.trimble.com/realworks.shtml.

